Rewetting Effects and Droplet Motion on Partially Wetted Powder Surfaces

Karen P. Hapgood, Thanh H. Nguyen, and Sunarko Hauw
Dept. of Chemical Engineering, Monash Advanced Particle Engineering Laboratory, Monash University, VIC
3800, Australia

Simon M. Iveson
Dept. of Chemical Engineering, University of Newcastle, Callaghan NSW 2308, Australia

Wei Shen
Dept. of Chemical Engineering, Australasian Pulp and Paper Institute, Monash University, VIC 3800, Australia

In high shear mixer granulation, the powder is agitated in a vessel while liquid is sprayed onto the powder. Formation of "nuclei" can be predicted using a nucleation regime map. However, this approach assumes that only dry powder enters the spray zone. Industrial granulation processes commonly add 20–50 wt % fluid, and the partially wetted powder recirculates many times through the spray zone. The effect of partially wetted powder re-entering the spray zone is not currently known. To investigate, droplets were added to a powder bed at controlled separation distances and time intervals. A strong correlation between drop penetration time and droplet motion on the powder bed surface was observed. For fast penetrating systems, nucleation was only slightly affected by the presence of the previous droplet. However, systems with long penetration times showed lateral droplet motion due to Laplace pressure differences. Implications for the nucleation regime map are discussed. © 2009 American Institute of Chemical Engineers *AIChE J,* 55: 1402–1415, 2009
Keywords: granulation, nucleation, drop penetration, wetting, spreading, powder

Introduction

Wet granulation is a size enlargement process aimed at improving a powder's properties.[1] The wet granulation process exhibits three main stages which can occur simultaneously in a high-shear granulator: wetting and nucleation, consolidation and growth, and granule attrition and breakage.[2]

This article considers the wetting and nucleation stage (shown schematically in Figure 1), which involves a liquid binder being sprayed onto the powder bed surface from a nozzle. In the high shear mixers used by the pharmaceutical, food and detergent industries, the powder is agitated in a vessel while liquid is sprayed onto the powder from above. The drops impact the powder surface, wet and penetrate into the powder to form the initial granules or "nuclei". The concentration of binder in the nucleus is dispersed by attrition and breakage through mechanical mixing.

If the binder does not wet the powder easily, large highly saturated granules will be produced.[1] Hence, nucleation is dependent on the drop penetration time[3] and the interaction with other droplets at high dimensionless spray flux.[4]

The dimensionless spray flux parameter Ψ_a[5] can be used to describe the spray density and initial nuclei size distribution of nuclei formed in the spray zone. The spray flux parameter also forms part of the nucleation regime map, which describes the conditions for good nucleation.[4] Ideally,
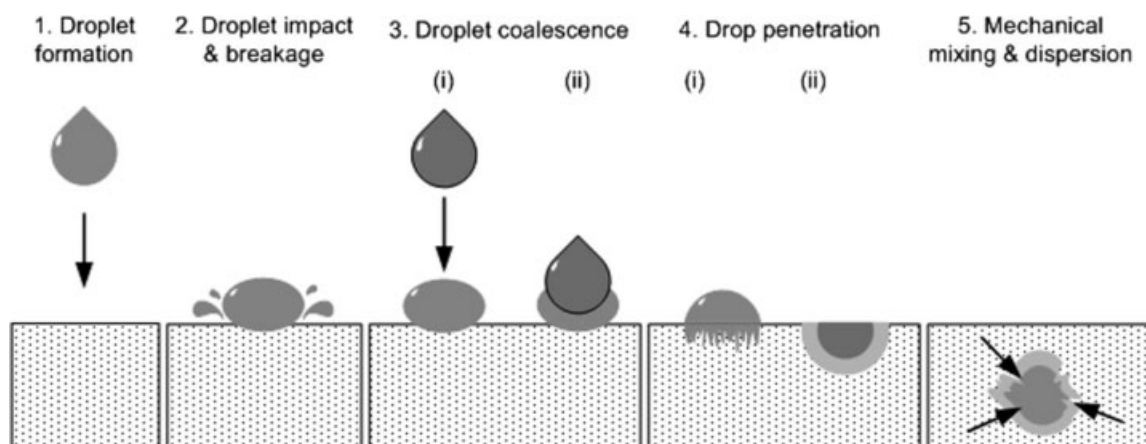
Figure 1. Five steps of nucleation (redrawn from Hapgood et al.[4]).

nucleation occurs in the drop controlled nucleation regime, each drop forms a single nucleus granule, which occurs at low spray flux and low drop penetration time.[4] The spray flux concept has been applied to drum granulation,[6] modeling[7,8] and scale-up of granulation.[9–13]

However, dimensionless spray flux has been validated using only dry powder entering the spray zone. Industrial granulation processes commonly add 20–50 w/w % fluid to the granulator. This means that the partially wetted powder recirculates through the spray zone multiple times. The differences in granule properties formed from dry powder compared to a partially saturated powder are not currently known, but potential differences in nucleus size and liquid saturation are expected (see Figure 2). The aim of this project is to answer the following question: Is there is any difference between the outcomes of the following two scenarios?

(1) Two droplets simultaneously hit the powder bed surface to form nuclei which overlap (Figure 2a).

(2) One droplet hits the powder bed surface and overlaps with a nuclei formed on a previous pass through the spray zone (Figure 2b).

When do two overlapping droplets form two nuclei as per Figure 2a and when do the droplets combine to form one larger nucleus? (See Figure 2b). Nucleation of a partially wet powder bed has not been studied previously, although it is expected to depend on the separation distance between the two droplets, drop spreading on the surface, the nucleation ratio and the drop penetration time. This paper uses single droplet nucleation experiments for several fluid-powder combinations at controlled separation distances and time intervals to study the nucleation behavior of partially wetted powders.

Experimental

Materials characterization

Glass ballotini powders, lactose monohydrate, calcinated alumina (CA300, Unimin), polyethylene glycol (Sigma-Aldrich) and glycerol (Sigma-Aldrich) were chosen to study nucleation behavior. Four grades of glass ballotini powders (AC, AE, AG, and AH, Potter Industries, Laverton Australia) were used together with two different size distributions of lactose (100 mesh and 200 mesh, denoted by L1M and L2M respectively, Wyndale, New Zealand). All powders were used "as received".

Four polyethylene glycols (PEG) with differing molecular weights were used to vary the fluid viscosity (PEG200, 300, 400, and 600). Several glycerol-water solutions were used (40, 60, 80, and 100% glycerol) to vary the fluid properties. A small amount of food dye was added to the liquids to assist observations of droplet motion. Glass ballotini and alumina are insoluble in all the fluids, although lactose was
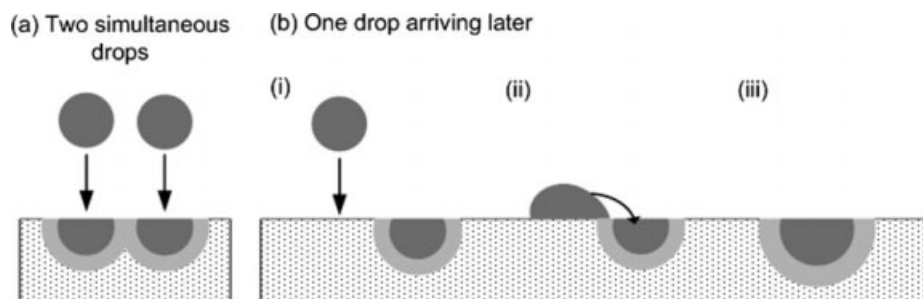

Figure 2. Comparison of possible behaviors of two droplets.

Dark gray area represents highly saturated region formed during drop penetration, and the lighter gray region represents less saturated powder that was wetted during subsequent spreading of the drop through the powder bed.

Table 1. Powder Properties Summary

Powder	Grade	Min. Size (μm)	Max. Size (μm)	True Particle Density (g/cm^3)
	AC	125	250	2.47
Glass	AE	90	150	2.47
Ballotini	AG	53	125	2.47
	AH	45	90	2.47
Lactose	100 mesh	75	250	1.54
Monohydrate	200 mesh	75	180	1.54
Calcinated alumina	N/A		45	3.9

soluble in the glycerol-water solutions. Since the experiment was completed within a few seconds, we believe that any dissolution of the lactose into the glycerol-water solutions would have been minimal and with minimal effect on our results. Powder properties based on vendor specifications are given in Table 1. Table 2 summarizes the liquid properties (based on data from CRC Handbook of Chemistry and Physics or the vendor).

Experimental set-up and procedure

The experiments were carried out by sieving the powder through a 1.40 mm sieve into a petridish to create a loosely packed powder bed. The surface of the powder bed was scraped smooth by using a metal ruler. The powder weight added to each dish was recorded to calculate the bed porosity.[3] A 1 ml syringe with 21 gauge needle was used to drop the liquid binder onto the powder bed. The syringe was clamped onto the needle rod, which could be translated to give varying separation distance between droplets, thus varying the simulated spray flux. Experiments were conducted at room temperature (25°C) to avoid solidification of PEG600. A stopwatch was used to measure the time interval between the first and second droplets. A schematic diagram of the experimental set-up is shown in Figure 3.

The first droplet was released from a height of ~1 mm and landed gently onto the powder bed and the penetration time was recorded. The syringe needle was then shifted across to the desired separation distance, which varied from 1 to 5 mm (measured centre to centre). The time interval between droplets was between 30 s and 1 h, and was approximately twice the drop penetration time of each powder-liquid combination. When the time interval was reached, the second droplet was released onto the powder bed. The wetting and penetration behavior of the second droplet in the presence of the first droplet was observed and the number of nuclei formed from

Table 2. Liquid Binder Properties at 25°C

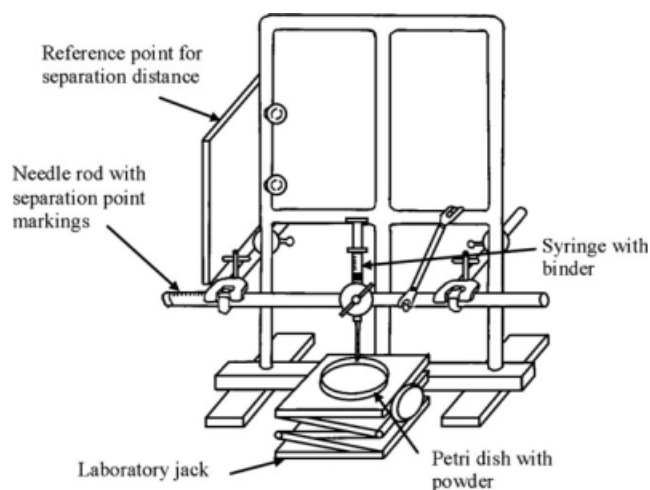| Fluid	Viscosity μ [mPa s]	Surface Tension γ [mN/m]	μ/γ
PEG200	60	43.7	1.4
PEG300	95	43.7	2.2
PEG400	120	43.7	2.7
PEG600	150–190	44.5	3.8
Glycerol	934	62.5	14.9
80 wt % glycerol	59.9	65.7	0.9
60 wt % glycerol	10.7	66.9	0.2
40 wt % glycerol	3.7	67.9	0.1

Figure 3. Experimental setup.

two droplets was recorded, based on the visual observations. The petridish was then rotated and this procedure was repeated until at least six replicates were produced on the petridish. Selected experiments were filmed using a digital camera and optical microscope to observe the droplet behavior. Nuclei were then separated from the dry powder by sieving. The number and type of nuclei present were recorded together with the nuclei size. The nucleation ratio K was calculated as the ratio between the drop diameter and the nuclei diameter.

Results

Effect of powder and binder properties on nucleation behavior

The particle size of the powder and the viscosity of the liquid can significantly alter the drop penetration time.[3] Drop penetration times t_p were recorded for a droplet penetrating into the dry powder bed and the results are summarized in Table 3. The values represent an average of either 12 or 24 measurements. The bed porosity ε of the glass ballotini is fairly consistent for each grade (varying from 0.45 to 0.49 for all grades), while for industrial powders the bed porosity varies from 0.63 to 0.65 for lactose 100 mesh, 0.71–0.74 for lactose 200 mesh and 0.83–0.85 for calcinated alumina. The binder droplet volume also varies for each type of binder used. For the PEG binders, the droplet volume V_0 can vary from 7.6 to 10.5 μl, while for the aqueous glycerol solutions, the droplet volume varies from 1.2 to 1.5 μl. Table 3 shows that the drop penetration time is faster for larger particles and lower viscosity binders, which agrees with previous work.[3]

In the drop penetration time experiments, three possible nuclei morphologies were identified:

(a) A single nucleus would be formed from two droplets, either due to a small separation distance and/or movement of the second droplet into the crater of the first.

(b) Two separate nuclei would be formed.

(c) "Dumbbell" shaped nuclei, where the droplets partially merged together.

There is a strong correlation between the separation distance and the observed nuclei morphology. At short

Table 3. Drop Penetration Time Summary (Initial Drop Only)

Powder	Binder	n	ε	V_o (μl)	t_p (secs)
AC ballotini	PEG200	24	0.45	9.8	2
	PEG300	24	0.45	10.0	3
	PEG400	18	0.45	10.5	5
	PEG600	18	0.45	10.3	6
AE ballotini	PEG200	18	0.47	9.8	3
	PEG300	12	0.47	10.0	4
	PEG400	24	0.47	10.5	6
	PEG600	18	0.48	10.3	9
	Glycerol	18	0.48	1.5	43
	80 wt % Gly	18	0.48	1.4	6.5
	60 wt % Gly	18	0.47	1.2	1.6
AG ballotini	PEG200	24	0.49	9.8	5
	PEG300	18	0.48	10.0	8
	PEG400	24	0.48	10.5	10
	PEG600	18	0.48	10.3	16
	Glycerol	18	0.48	1.5	61
	80 wt % Gly	18	0.48	1.4	7.9
	60 wt % Gly	18	0.49	1.2	3.9
	40 wt % Gly	18	0.49	1.3	1.8
AH ballotini	PEG200	24	0.47	9.8	5
	PEG300	18	0.47	10.0	7
	PEG400	24	0.47	10.5	9
	PEG600	18	0.47	10.3	15
	80 wt % Gly	18	0.48	1.4	4.2
	60 wt % Gly	18	0.49	1.2	2.3
Lactose 100 mesh	PEG200	18	0.63	8.0	12.6
	PEG300	18	0.65	7.6	14.6
	PEG400	18	0.64	7.7	21.5
	Glycerol	18	0.64	1.5	123
	80 wt % Gly	18	0.65	1.4	55
	60 wt % Gly	18	0.64	1.2	8.8
	40 wt % Gly	18	0.63	1.3	3.4
Lactose 200 mesh	PEG200	18	0.74	8.0	48
	PEG300	18	0.74	7.6	66
	PEG400	18	0.74	7.7	81
	Glycerol	18	0.73	1.5	447
	80 wt % Gly	18	0.71	1.4	88
	60 wt %Gly	18	0.72	1.2	23.3
	40 wt % Gly	18	0.72	1.3	10.8
Calcinated alumina	PEG200	18	0.83	8.0	118
	PEG300	18	0.83	7.6	149
	PEG400	18	0.84	7.7	188
	Glycerol	18	0.84	1.5	1133
	80 wt % Gly	18	0.84	1.4	250
	60 wt % Gly	18	0.85	1.2	79
	40 wt % Gly	18	0.84	1.3	12

Where n, number of replicates; ε, bed porosity; V_0, drop volume; t_p, average penetration time.

separation distances (1–2 mm) a single nucleus is more likely to be formed as the second droplet penetrates into the first droplet to form a single nucleus (double sized). At long separation distances, two separate nuclei are formed. For intermediate separation distances, which we refer to as the "critical range of separation distance," a single-centred nucleus is formed, but two types of nuclei morphology can be observed. One type is where the second droplet flows directly into the first droplet and the second case is when the second droplet lands adjacent to the first droplet, but after a short period of ~1 s, lateral droplet motion can be seen by the second droplet into the first droplet, possibly due to a Laplace driving force (see "Discussion" section for an explanation). When one nucleus is formed, an imprint is left by the second droplet as it flows into the first droplet, as shown in Table 4.

Effect of separation distance and time interval

The relationship of the nuclei morphology as a function of the time interval between the two droplets and the separation distance are presented in Figures 4 and 5 for lactose 200 mesh with binders PEG200 and PEG400 respectively. Each point on the graph represents the average of six measurements. The error bars show the estimated error in separation distance to be constant at ±0.5 millimetres.

The percentage of granules that form two nuclei was determined using the visual overhead observations of droplet behavior. The percentage of two nuclei granules formed was defined as the chance of two nuclei formed for a given separation distance. When the number of nuclei formed was always one, then the chance of two nuclei forming is zero percent, while the percentage is hundred percent when two nuclei are always formed. For a dumbbell shaped granule, it was assumed that there was an equal chance that the granule would form one nucleus or two nuclei (in reality, this probability depends on the strength of the dumbbell bond and the shear conditions in the granulator). In this manner the percentage two nuclei formed was calculated for each powder-binder combination from the experimental results. Each result is the average percentage of nuclei formed, based on 18–24 replicate nucleation experiments.

From Figures 4 and 5, there are a low percentage of two nuclei forming at a separation distance of 0 and 1 mm. Aside from one outlier, the percentage of two nuclei forming increases steadily between 2 and 4 millimetres, until the percentage reaches a 100% at 4 or 5 mm. This trend makes intuitive sense.
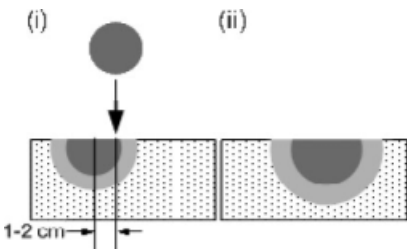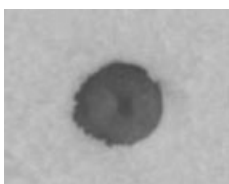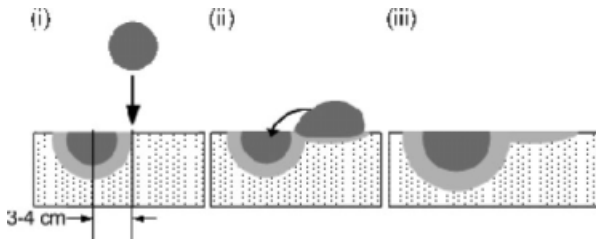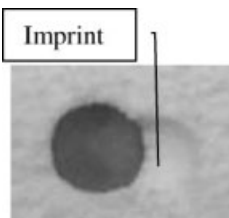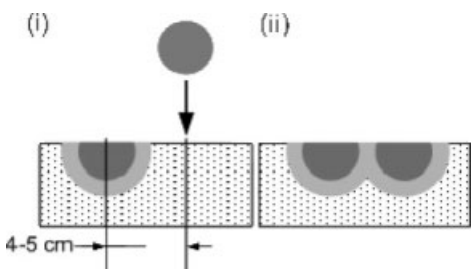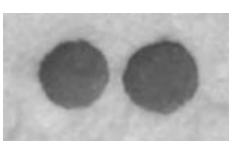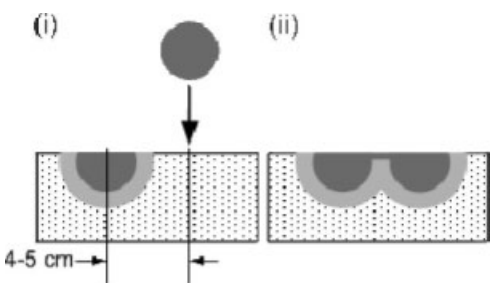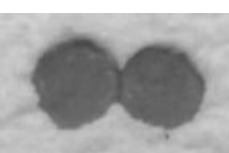
The other major observation from Figures 4 and 5 is that varying the delay time between droplets from 5 s to 1 h made very little difference. The drop penetration time in these two cases was 48 and 81 s respectively (Table 3). So when the delay time was only 5 or 30 s, this means that the first droplet was still visible at the powder surface when the second droplet landed. It might be expected that if the first droplet had already fully soaked into the powder then this pre-established wet zone would be more likely to cause lateral motion of the second droplet, thus reducing the probability of forming two separate nuclei. However, there was no indication of this.

Effect of powder and liquid properties

Figures 6–9 plot the percentage of two nuclei as a function of the interdrop separation distance for several powder-liquid combinations. The time interval varied from 30 s to 10 min (at least twice the drop penetration time) for experimental convenience. Error bars indicate the time interval accuracy of ±1 s and the standard error of the mean of the calculated percentage of two nuclei formed.

For all combinations of powder and binder used, a single nucleus was formed at 1–2 mm separation distance (0% two nuclei). At a separation distance of five millimetres, two separate nuclei were formed for all combinations. However, for the critical separation range of 2–4 mm, either behavior might occur, depending on the powder-liquid combination used. Within this range the second droplet lands just adjacent to the prewetted powder (i.e., adjacent to the footprint of the

Table 4. Nuclei Morphology Summary

Nuclei Morphology	Nuclei Morphology Behavior	Experimental Picture
Single nucleus (formed due to small separation distance)	(i) (ii) ... 1-2 cm	
Single nucleus (formed due to lateral drop movement)	(i) (ii) (iii) ... 3-4 cm	Imprint
Two nuclei	(i) (ii) ... 4-5 cm	
Dumbbell nucleus (drops partially merged together)	(i) (ii) ... 4-5 cm	

first droplet) leading to the formation of either: one nucleus, two nuclei or a dumbbell nucleus, depending on the drop penetration time of the powder and binder combination used.

Figures 6–9 show that the dominant effect on whether one nucleus or two nuclei are formed is the separation distance. For each powder-fluid combination, there is a critical separation distance where a modest effect of liquid properties (in particular, the viscosity) can be seen. There seemed to be a trend of increasing likelihood of nuclei coalescence with increasing binder viscosity. However, this effect is small compared to the experimental uncertainty. Therefore further experiments were performed at the critical separation distance for each powder. For glass ballotini, the critical separation distance occurs at 4 mm, while for lactose powders the critical separation distance can be taken as slightly smaller at 3 mm (the intermediate of 2 to 4 mm).

Reviewing the data in Figures 6–9 at the critical separation distance for each powder, a trend with increasing fluid viscosity can be seen. For example, Figure 6 shows that at 4 mm separation distance, reducing the fluid viscosity results in a higher percentage of two separate nuclei being formed. Further experiments investigating droplet motion were performed at these critical separation distances, to investigate these observations further.

Effect of drop penetration time

Figures 12–14 show the relationship between the drop penetration time and percentage of two nuclei for the glass ballotini, lactose and calcinated alumina powders respectively. The drop penetration experiments were performed at the critical separation distance for each powder at a time
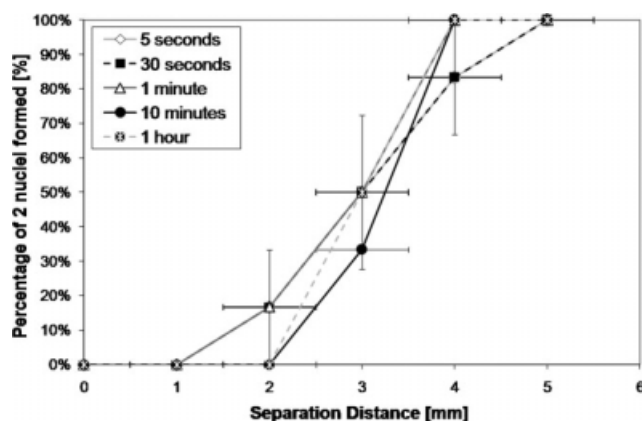
Figure 4. Percentage of two nuclei granules formed as a function of separation distance and time interval between two drops for lactose 200 mesh and PEG200.

Figure 6. Percentage of two nuclei granules formed as a function of separation distance between two drops for AC glass ballotini.

interval which was at least twice the drop penetration time (between 30 s and 10 min). Error bars represent the time interval accuracy of ±1 s and the standard error of the mean of the calculated percentage of two nuclei formed respectively.

From all powders, the percentage of two nuclei formed was inversely proportional to the drop penetration time. For systems with short drop penetration times, when the second droplet landed on the prewetted powder area, it immediately penetrated into the powder bed to form either a second, separate nucleus or a dumbbell nucleus. Thus, formation of two separate nuclei occurred more often. In contrast, for powder-fluid combinations with long drop penetration times the second droplet tended to move sideways and penetrate into the prewetted powder area, as shown in Figure 2b. Figures 10 and 11 show a sequence of images depicting the nuclei formation and lateral droplet motion on glass ballotini and lactose powder respectively.

For the glass ballotini powder, the PEG fluid data for all size grades collapses onto a single curve although the PEG
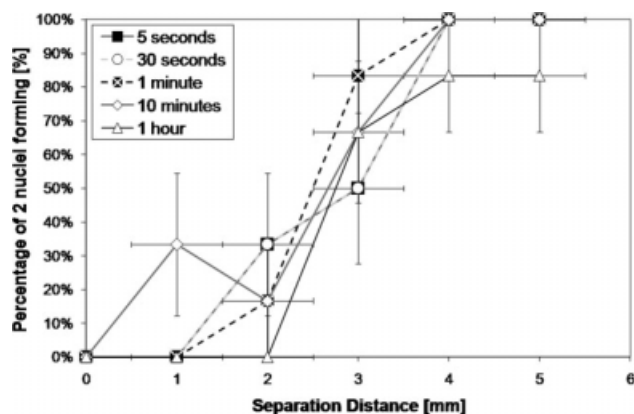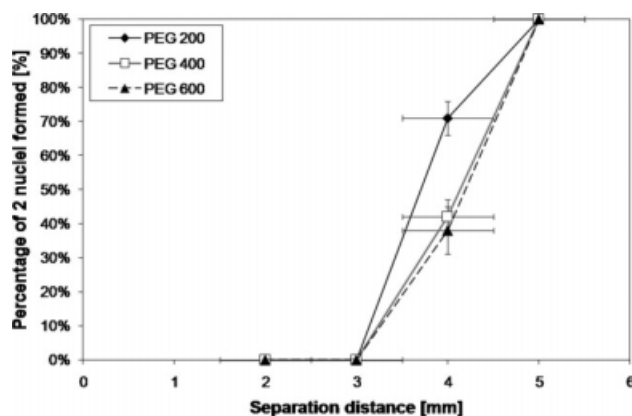
and glycerol solution data do not overlap (refer to Figures 12a,b respectively). The two lactose grades (100 and 200 mesh) formed separate families of curves (Figures 13a, b) while the fluid used had only a minor effect. This is possibly due to the differences in bed porosity and packing structure of these two powders which affects the drop penetration behavior.[3] Different fluids created different curves, due to differences in the initial droplet sizes (refer to Table 3) and differences in the rates of wetting and spreading on surface, which results in different sensitivity to separation distance. Data for alumina (Figure 14) also seemed to show separated curves for glycerol and PEG experiments.

Drop penetration time of the first and second droplets

The drop penetration time of the first and second droplets impacting on the powder bed were measured to investigate the effect of rewetting on the drop penetration time. The experiments were performed with a time interval of between 30 s and 10 min, depending on the binder used (the time interval was at least twice the drop penetration time for complete nucleation). The drop penetration times for the first and second droplets are shown in Figure 15.
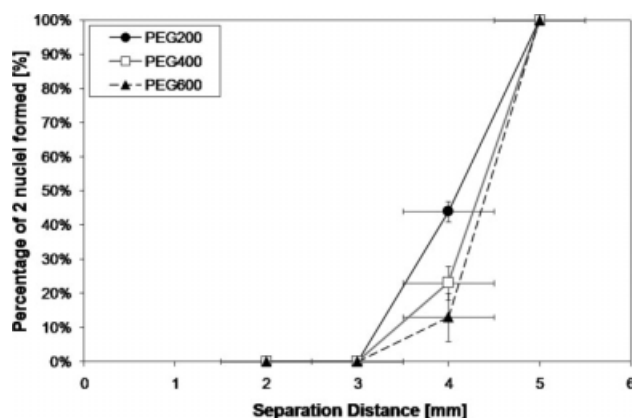

Figure 5. Percentage of two nuclei granules formed as a function of separation distance and time interval between two drops for lactose 200 mesh and PEG400.

Figure 7. Percentage of two nuclei granules formed as a function of separation distance between two drops for AH glass ballotini.

Figure 8. Percentage of two nuclei granules formed as a function of separation distance between two drops for lactose 100 mesh.
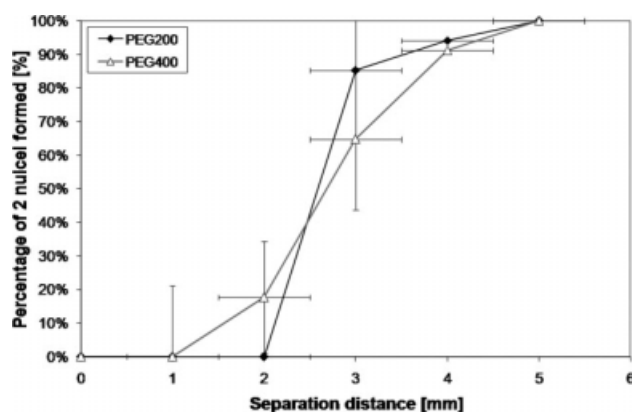

Figure 9. Percentage of two nuclei granules formed as a function of separation distance between two drops for lactose 200 mesh.

Figure 15 shows that the drop penetration time of the second droplet is shorter than for the first droplet on 100% dry powder. This is consistent with previous work where the drop penetration time decreased as the saturation of the powder bed increased.[14] The second droplet takes less time to penetrate in the presence of the first droplet, and the reduction in penetration time increases as the penetration time increases However, it can be seen that the penetration times for lactose systems do not portray a linear relationship between the first and second drop penetration times and fits better to a power function.

Discussion

Initiation of the penetration

Liquid penetration into a capillary system will occur if the solid surface of capillary has a thermodynamic contact angle smaller than 90°. This is a prerequisite for conventional droplet sizes, since the driving force for capillary penetration (the Laplace pressure) is positive only when the thermodynamic contact angle is smaller than 90°.[15] When a liquid droplet is introduced onto a powder bed, an apparent contact angle 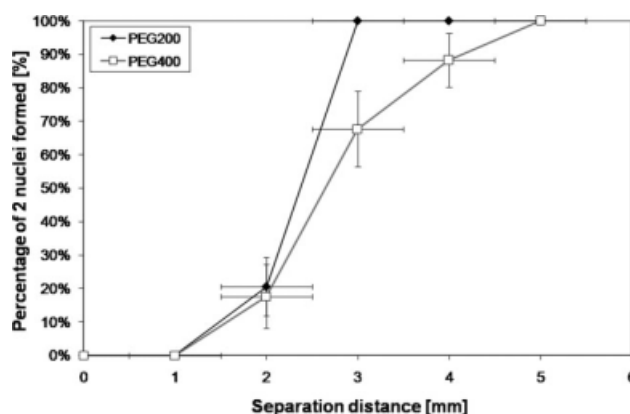can be observed. In most cases, if not all, this apparent contact angle is not the thermodynamic contact angle, but larger than it due to surface roughness. Figures 13 and 14 show that liquids having >90° apparent contact angles can still penetrate into powder beds. Clearly, the thermodynamic contact angles that drove the liquid penetration in those situations must be smaller than 90°. Time is required for the penetration front to adopt the thermodynamic contact angle. Also, in the beginning of wetting, a microscopic liquid spreading precursor at the liquid/solid contact line must be first formed to facilitate the advancement of the macroscopic contact angle.[16] These factors, together with the development of penetration resistance in a capillary system once capillary flow starts, are responsible for the different wetting behavior on dry and partially wetted powder beds.

Drop penetration behavior on dry and partially wet powder beds

Our results show that the penetration behavior of the second droplet at the critical separation distance from the footprint of the first droplet strongly influences the wetting morphology. For fast penetration systems, the wetting behavior of the second droplet was only slightly affected by the presence of the previous droplet, but for slow penetration
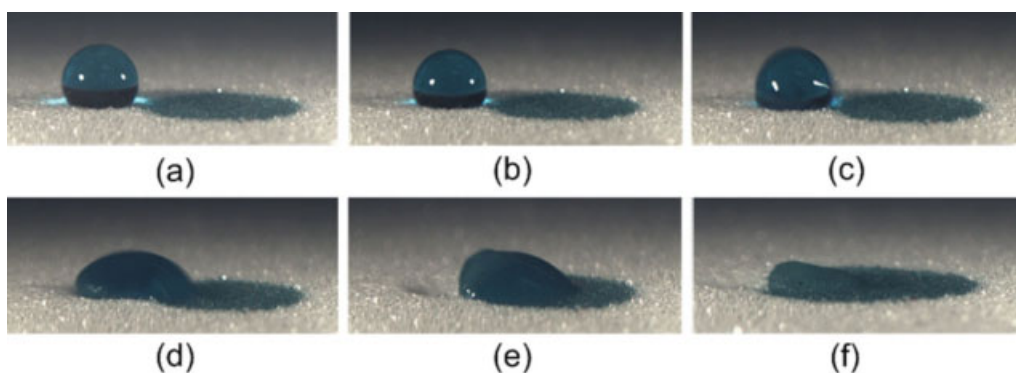

Figure 10. Adding a drop of PEG400 to prewetted AH glass ballotini powder.

The pictures are taken at (a) impact, (b) 0.94 s after impact, (c) 0.95 s, (d) 0.96 s, (e) 1.01 s, and (f) 6.97 s. The footprint of the previous drop is visible to the right of the added drop (critical separation distance of 4 mm). [Color figure can be viewed in the online issue, which is available at www.interscience.wiley.com.]
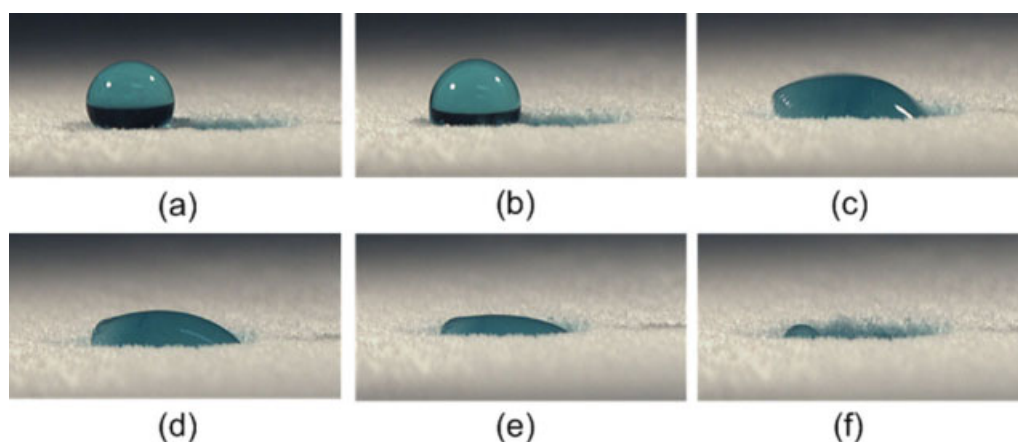
Figure 11. Adding a drop of PEG400 to prewetted lactose 200 mesh powder.

The pictures are taken at (a) impact, (b) 4.05 s after impact, (c) 5 s, (d) 5.02 s, (e) 12.06 s, and (f) 51.6 s. The footprint of the previous drop is visible to the right of the added drop (critical separation distance of 3 mm). [Color figure can be viewed in the online issue, which is available at www.interscience.wiley.com.]

systems, much more significantly. The key differences in droplet behavior for these two cases are illustrated in Figures 16 and 17.

For fast penetration systems, the second droplet penetrates into the dry powder bed, instead of merging with the first droplet and penetrating into the footprint of the first droplet (see Figure 18). The reasons for this are as follows: Firstly, for a fast penetration liquid, the time required for establishing the wetting precursor film[16] is much shorter, and formation of the precursor film may not be the limiting step. However, for a slow penetration liquid, the formation of the precursor film could be much longer. Secondly, in a fast penetrating system, the second droplet wets and penetrates the powder bed rapidly. This enables the droplet to penetrate into the powder bed to a reasonable depth within a very short period of time. The depletion of the droplet volume

above the powder bed is rapid and the apparent contact angle between the droplet and the powder bed surface also decreases rapidly. It is therefore difficult for the droplet to be in the situation described in Figure 19(3), where unequal contact angles on both sides of the droplet generate an imbalanced Laplace pressure which pushes the second droplet into the footprint of the first droplet (a special circumstance presented in Figure 10 will be discussed later). In essence, for fast penetrating systems, the rate of penetration into the dry powder bed is much faster than the rate of spreading over the powder surface. Thirdly, a dry powder bed presents a lower penetration resistance than the prewetted powder bed where pores have already been saturated by the liquid. Therefore drop penetration will occur predominantly in the dry region rather than in the wet region, even in circumstances where the second droplet has established
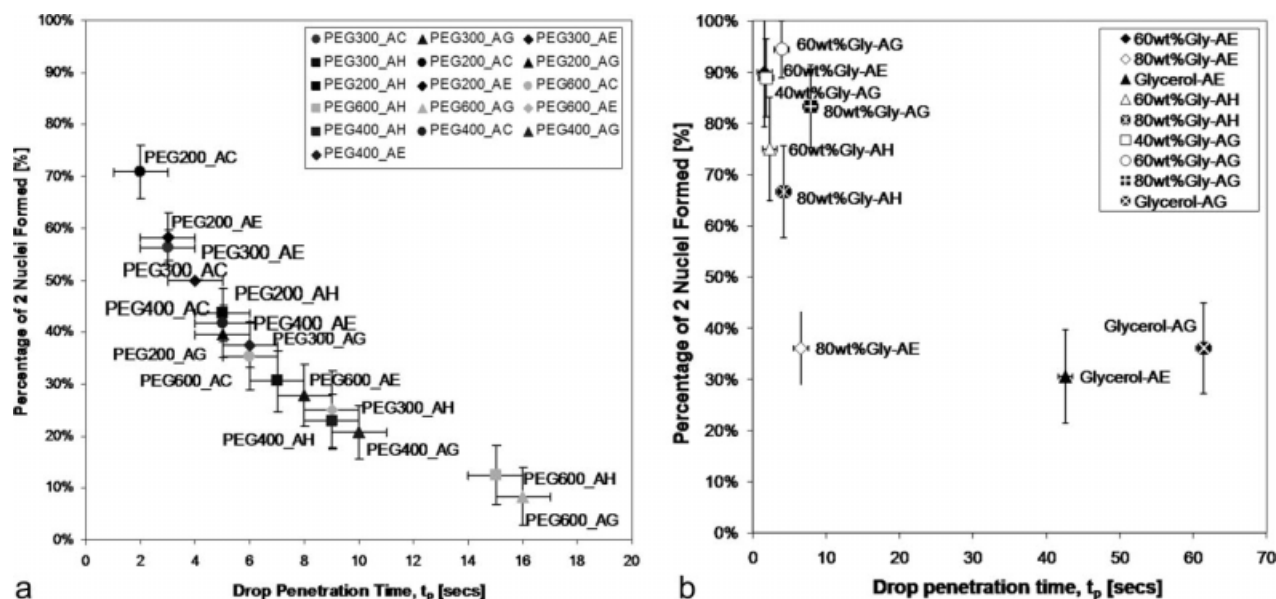

Figure 12. Number of nuclei formed for glass ballotini powders as a function of drop penetration time.

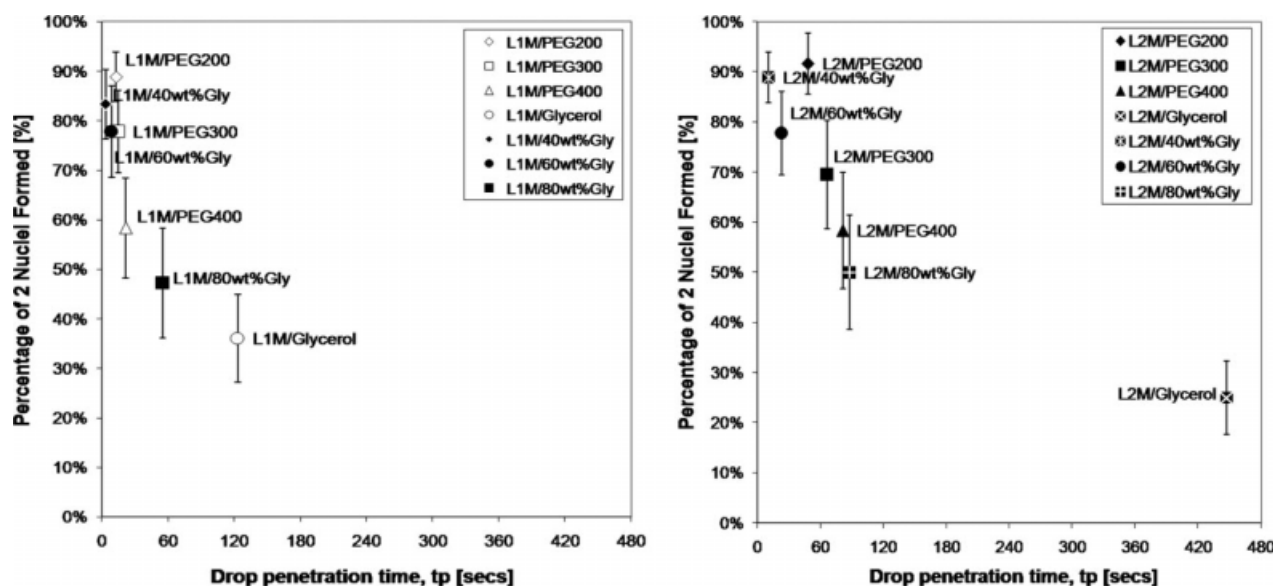(a) PEG fluids, (b) glycerol/water solutions (critical separation distance of 4 mm).

Figure 13. Number of nuclei formed as a function of drop penetration time for (a) lactose 100 and (b) 200 mesh powders (critical distance of 3 mm).

contact with the first droplet, but such contact has not triggered the lateral drop-merging movement.

These experimental observations that liquid penetration on a dry powder bed is faster than on a prewetted bed, can be backed up by theoretical descriptions of liquid penetration into powders. Middleman[17] considered liquid penetration into a porous medium with a capillary bundle model, and modelled the average velocity of flow into a single capillary using the Washburn model:

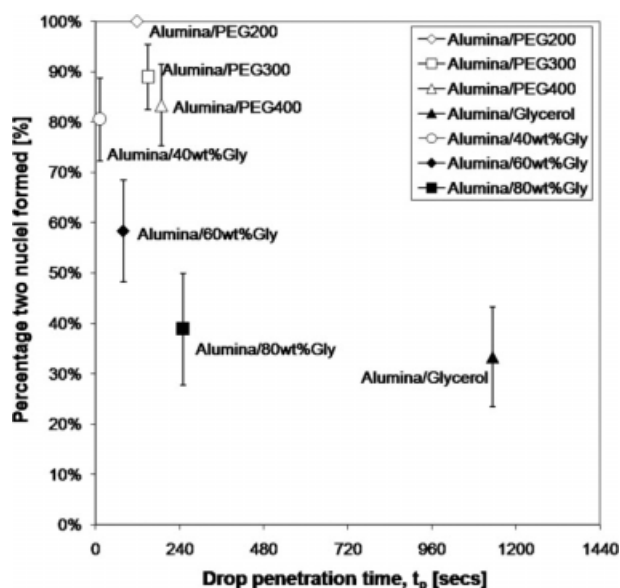$$\frac{dz}{dt} = \sqrt{\frac{\gamma_{LV}R\cos\theta}{8\mu t}} \qquad (1)$$

where z is the penetration distance, t is time, γ_{LV} and μ are the surface tension and the viscosity of the liquid, R is the equivalent pore radius and θ is the thermodynamic contact angle. Integrating Eq. 1 leads to Eq. 2:

$$z = \sqrt{\frac{\gamma_{LV}R\cos\theta}{2\mu}t} \ \text{ or } \sqrt{t} = z\sqrt{\frac{2\mu}{\gamma_{LV}R\cos\theta}} \qquad (2)$$

The volume V of a penetrating droplet sitting on a porous surface reduces with time:

Figure 14. Number of nuclei formed as a function of drop penetration time for calcinated alumina powders (critical distance of 3 mm).
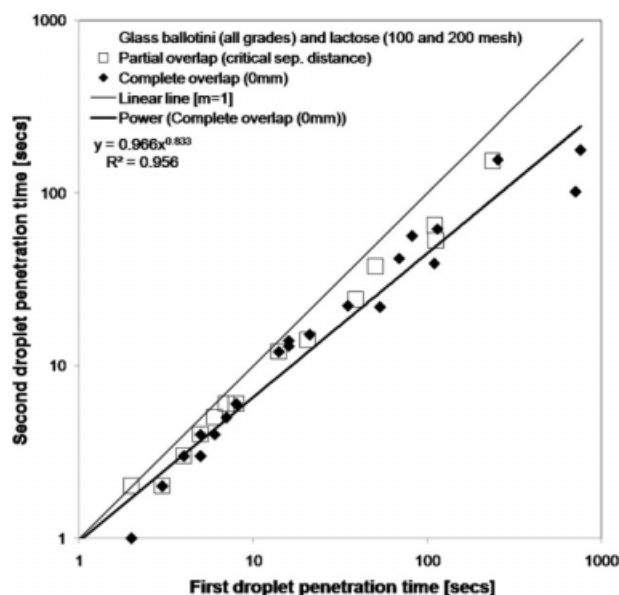

Figure 15. Drop penetration time of the first and second droplets for glass ballotini (AC, AE, AG, and AH grades) and lactose (100 and 200 mesh) powders.
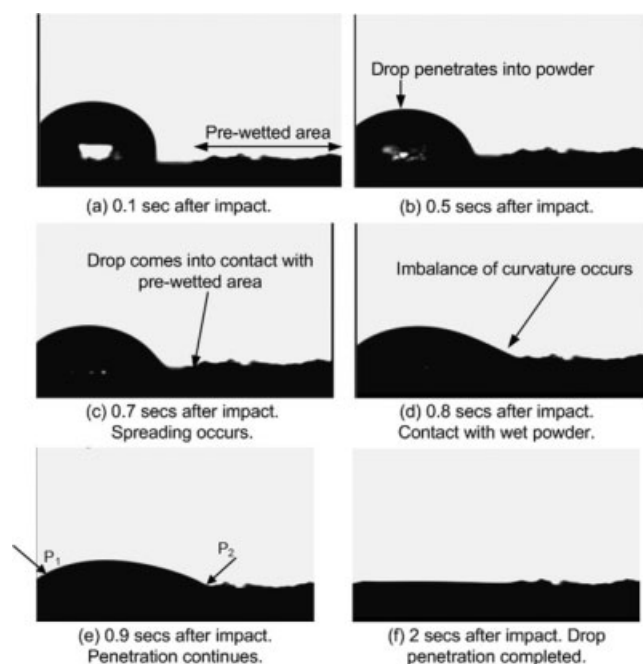
Figure 16. PEG 200 on AC ballotini powder.

Drop penetration time is 2 s with a separation distance of 4 mm.

Figure 17. PEG 400 on AG ballotini.

Drop penetration time is 8 s with a separation distance of 4 mm.

$$V(t) = V_0 - \pi R_d \varepsilon \sqrt{\frac{\gamma_{LV} R \cos \theta}{2\mu} t} \qquad (3)$$

where V_0 is the initial droplet volume above the porous surface, R_d is radius of the contacting circle of the droplet with the porous surface, ε is the porosity. The volume penetration rate into the porous media can then be written as:

$$-\frac{dV(t)}{dt} = \pi R_d \varepsilon \sqrt{\frac{\gamma_{LV} R \cos \theta}{8\mu t}} \qquad (4)$$

Substituting Eq. 2 into Eq. 4 leads to Eq. 5:

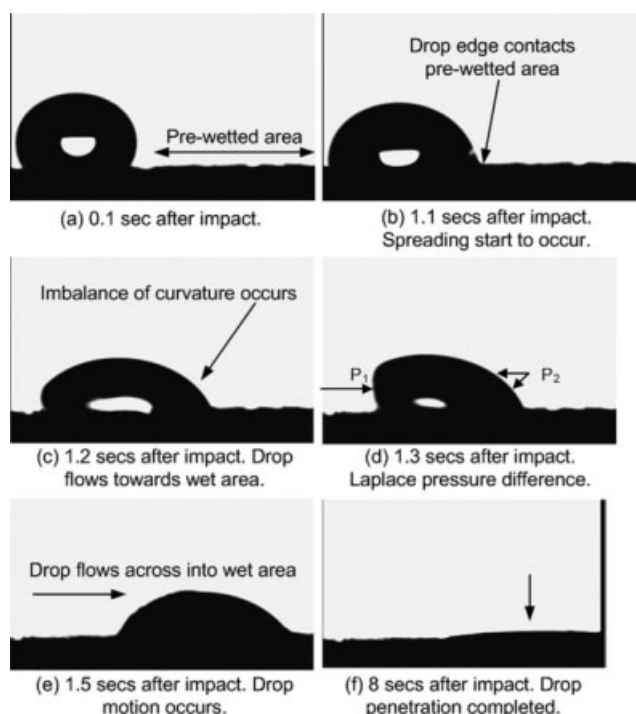$$-\frac{dV(t)}{dt} = \pi R_d \varepsilon \frac{\gamma_{LV} R \cos \theta}{4\mu z} \qquad (5)$$

Equation 5 shows that the penetration rate will slow down as the penetration depth z increases. Although the driving force ($\gamma_{LV}\cos\theta$) is constant, the flow resistance in a capillary increases as its filled length increases.

Equation 5 shows that liquid penetration on a dry powder bed is faster than on a prewetted bed where pores have been filled up to a certain degree, provided that the formation of the wetting precursor is not the limiting step. Thus, it explains why a fast penetrating liquid droplet penetrates into a porous media predominantly from the dry area and is not strongly influenced by the existence of the first one. This is supported by the nuclei formation data (Figures 10–12) and by the almost identical penetration times for the first and second droplets (Figure 15).
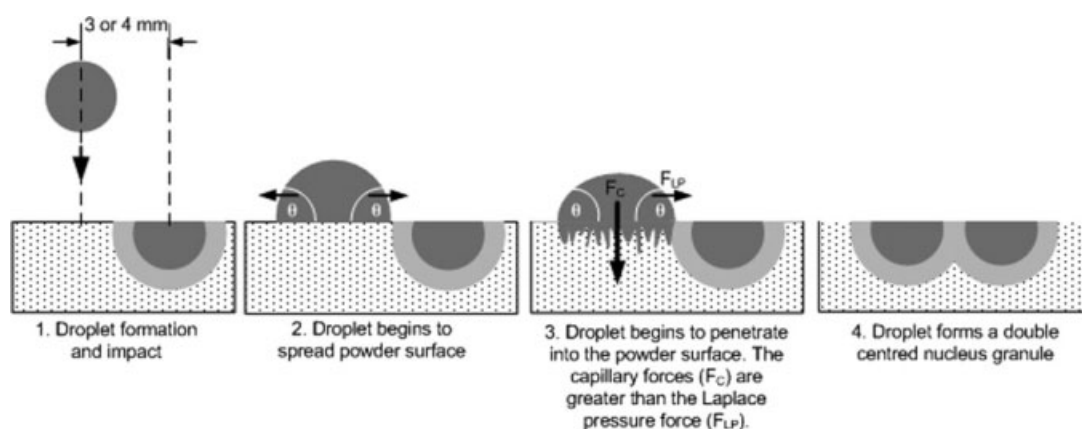

Figure 18. Schematic diagram of nucleation of a partially-wetted powder bed for a fast penetrating system.
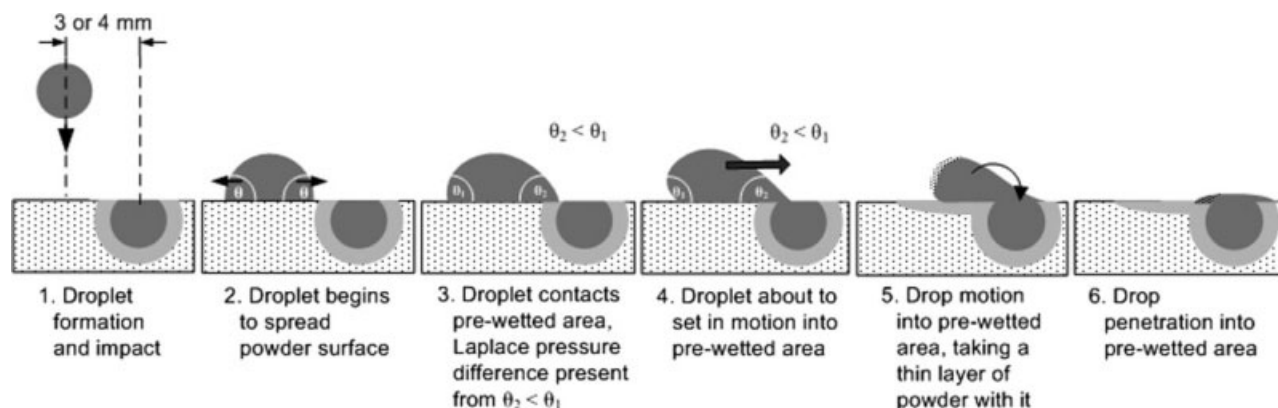
Figure 19. Schematic diagram of the lateral drop motion for a slow penetrating system due to Laplace pressure imbalance.

It is understandable that the formation of wetting precursor is slow and likely to be the limiting step for slow penetrating liquids. These liquids penetrate faster on a partially wetted porous surface where a precursor has already formed. Therefore the existence of the first droplet more significantly influences the penetration time of the second droplet. Because of the slow formation of wetting precursor on dry powder surface, the second droplet is more likely to be in a situation described in Figure 19(3), when it is placed near the footprint of the first droplet. The imbalanced Laplace pressure will generate a lateral force onto the droplet as it contacts the footprint of the first droplet (see Figure 17d). As the droplet moves laterally towards the first droplet, failure occurs at the powder–powder interface and a thin layer of powder adhered to the droplet base is carried across to the prewetted area. This leaves an imprint of the impact of the second droplet on the powder surface (Figure 19). This causes the penetration time of the second droplet to be slightly faster than the time needed for the original droplet, as the precursor film is established quickly on the prewetted powder area (see Figure 15).

It is possible also for the second droplet of fast penetrating liquid to merge into the footprint of the first droplet, although it is much less likely compared with the slow penetrating liquids. If the second droplet contacts the first droplet at a time where the penetration of the second drop has not advanced greatly, there is a chance that the Laplace pressure triggers the lateral movement of the droplet. Such a process has been captured in Figure 13. However, the likelihood of the lateral movement of the second droplet is much greater for the slow penetrating systems.

Predicting droplet migration

Larger droplets, droplets which spread to create a larger footprint, and powder-binder combinations with a larger nucleation ratio are expected to be more likely to move laterally and penetrate into a prewetted area. The ratio of droplet separation distance to nucleus size should appear in a nondimensional group on the *x*-axis of Figures 4–9. Drop migration is expected to occur when the centre-to-centre distance of the drops is less than the diameter of the nuclei. We define a critical separation distance, L^*, as the separation distance at which there is a 50% probability of drop migration to form a single nucleus. Assuming that all the nuclei formed are spherical, L^*

should be proportional to $d_{drop}*K$, where K is the nucleation ratio (expressed as diameter of the nuclei compared to diameter of the droplet used in its formation). Table 5 summarizes the experimentally measured nucleation ratios for PEG fluids on selected powders and the critical separation distance L^*, which was estimated for these powder-fluid combinations using Figures 4–9. Table 5 shows that penetration time t_p, nucleation ratio K and the 50% probability separation distance L^* are inter-related, but which (if any) of these is the cause and which are the effects cannot be determined at this time.

Figure 20 shows that as the nucleation ratio decreases, L^* increases. This trend seemed to be counter-intuitive—as the nucleus size decreases, it would be reasonable to expect that the second droplet would need to be placed ever closer to the centre of the initial droplet in order for drop migration to occur. However, Figure 20 shows the opposite trend. We postulate that drop migration may be affected by both nuclei spreading below the powder surface and drop spreading above the powder surface. For slow penetrating droplets, the dominant mechanism controlling L^* is the spreading of the droplet above the powder surface, whereas K is controlled by what happens below the powder surface. For high viscosity fluids, the slow droplet penetration means that they spend more time on the powder surface and hence are more likely to experience the differential Laplace pressure effect, causing them to migrate. Thus, increasing the fluid viscosity increases the penetration time and increases L^* by allowing more time for spreading and droplet migration. In contrast, the nucleation ratio is determined by the dynamics of wetting beneath the surface. In the powder bed, increasing viscosity acts to retard droplet spreading and reduce K. Further

Table 5. Summary of Rewetting and Nucleation Parameters for Selected Powder-Liquid Combinations

Powder	Binder	t_p (secs)	L^* (mm)	K (mm/mm)
Lactose	PEG200	12.6	2.5	4.0
100 mesh	PEG300	14.6	2.7	3.6
	PEG400	21.5	2.9	3.2
Lactose	PEG200	48	2.3	6.5
200 mesh	PEG300	66	2.6	5.9
	PEG400	81	2.7	5.2
AH	PEG200	5	4	1.7
ballotini	PEG600	15	4.2	2.4

t_p, average penetration time; K, nucleation ratio; L^*, separation distance corresponding to 50% drop migration probability.
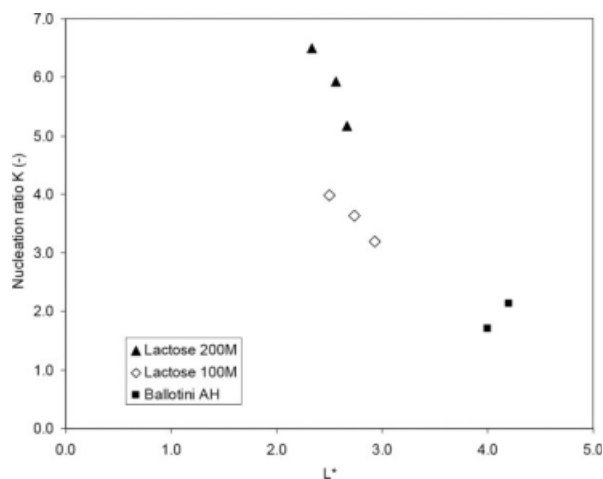
Figure 20. Relationship between the nucleation ratio K and L* (separation distance with 50% probability of drop migration) for selected powder-fluid combinations.

Figure 21. 7 wt% HPC solution, $\psi_a = 0.51$.

The spray nozzle passed directly overhead and sprayed almost all of the viewing area, but lateral fluid motion of the slow penetrating system has revealed dry powder sections[14].

experiments to film the impacting, spreading and migrating of the second droplet are required to test this hypothesis before the trend observed in Figure 20 can be satisfactorily explained.

Implications for granulation

Short granulation experiments[14] showed evidence of lateral droplet motion with binders of long drop penetration time. Lactose (similar to the lactose 200 mesh used in this study) was granulated with 7 wt % HPC solution (viscosity = 105 cP) at a spray flux $\psi_a = 0.51$.[14] As shown in Figure 21, the HPC solution moved laterally leading to pooling of HPC and leaving segments of dry powder. The pooling behavior was not seen in the experiments with water, even at much higher spray flux. At the time the experiments were performed, the behavior could not be accurately explained. However the rewetting results in this paper provide an explanation for the lateral motion and liquid pooling of HPC, where binders with long drop penetration times (HPC has a drop penetration time
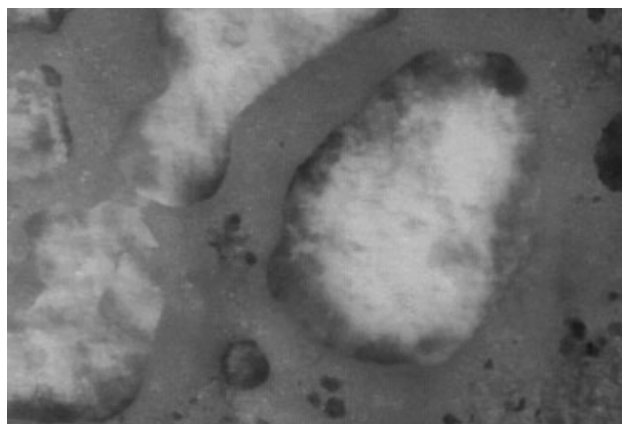
of ~2 min) have significant droplet lateral motion, due to differences in Laplace pressure of the droplets, compared with fast-penetration binders.

Rewetting has important implications for process design and control of industrial granulators. The overall aim of the nucleation stage is to distribute the liquid as uniformly as possible throughout the powder and form nuclei granules. The nucleation regime map recommends that fast penetrating powder/binder systems and low spray flux be used to achieve optimal liquid distribution and uniform nucleus properties, including size and saturation.[4] The results generated to date show that for fast penetrating systems, there will only be migration and merger of droplets on the powder surface at very short separation distances. In contrast, for systems with long penetration times, lateral motion of droplets towards prewetted areas will lead to local concentrations of binder fluid. These local concentrations will result in larger, highly saturated nuclei and a broader nuclei size distribution. This process is illustrated in Figure 22. Symptoms of this in
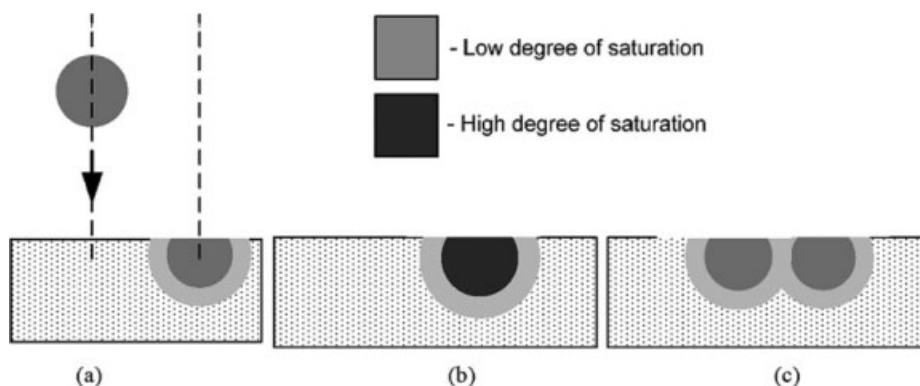

Figure 22. Schematic diagram of the degree of saturation for a single nucleus and a double-centerd nucleus granule.

(a) Droplet impact on partly saturated bed. (b) If drop penetration is slow, the droplet will migrate to form a larger and highly saturated nucleus. (c) If drop penetration is fast, the two separate nucleus with uniform size and saturation will be formed.
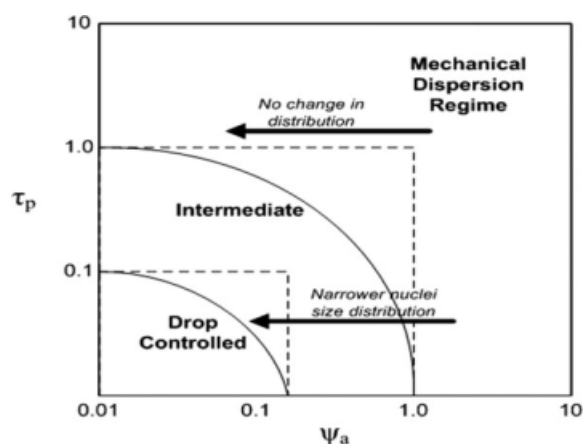
Figure 23. Nucleation regime map with the adjusted boundaries incorporating the drop migration in multi-pass spray flux.

Dotted lines represent original regime boundaries.[4]

industrial practice might include the production of large or oversized granules, which contain excessive binder. Production of larger than expected granules due to droplet migration has been observed in nucleation only granulator experiments[18] where powder-liquid combinations with short penetration times produced narrower nuclei size distributions compared to systems with long penetration times, even at the same low spray flux. Droplet migration and the formation of rivulets was observed to be the cause of the problem.[18] This implies that the spray flux for a formulation with a long penetration time needs to be even lower, to compensate for droplet motion and nuclei merger. Long penetration times mean that nucleation occurs in the mechanical dispersion regime,[4] where the mechanical mixing action in the granulator is the dominant influence on the dispersion of fluid through the powder. Fluid migration towards prewetted areas seems to be a significant effect on liquid distribution for in the mechanical dispersion regime and this needs to be incorporated into future models.

This work has shown that as the penetration time increases, the tendency for droplet migration increases, and a greater separation distance between droplets is required—thus the spray flux required to maintain drop controlled nucleation will decrease as the drop penetration time increases. This droplet migration behavior implies that the drop controlled regime boundary should be adjusted to become a function of the drop penetration time, as shown in Figure 23. The original nucleation regime map used arbitrary square regime boundaries, but the experimental validation of the nucleation regime map produced curved arcs,[4] similar to what we propose in Figure 23. The original experimental results[4] were performed by spraying over a period of time, and thus the spray droplets would have been added to a partially saturated powder bed, where rewetting and droplet migration would have occurred. Thus the original experimental validation corroborates the revised nucleation regime map with curved regime boundaries (as shown in Figure 23), and implies that droplet migration on partially wetted powder plays a significant role in liquid distribution.

Conclusions

Previous work on nucleation in the spray zone has only considered the first pass wetting of a dry powder. We have shown that for slowly penetrating liquids, the presence of nuclei from previous passes can have a large effect on the number of nuclei formed during subsequent passes through the spray zone. There is a tendency for droplets of these slow-penetrating liquids to have significant lateral droplet motion due to Laplace pressure differences and merge with the nuclei from previous passes. Hence nuclei fusion occurs more frequently than predicted by the dimensionless spray flux parameter resulting in a wider variation in both nuclei saturation and size distribution than previously expected. Droplet migration behavior implies that the drop controlled regime boundary should be adjusted to become a function of the drop penetration time, such that as the penetration time increases, the spray flux required to remain in the drop controlled regime is reduced.

Literature Cited

1. Litster JD, Ennis BJ. *The Science and Engineering and Granulation Processes*. Dordrecht: Kluwer Academic Publishers, 2004.
2. Ennis BJ, Litster JD. *Size reduction and size enlargement, in Perry's Chemical Engineers' Handbook*. Green D, editor. New York: McGraw-Hill. 1997.
3. Hapgood KP, Litster JD, Biggs SR, Howes T. Drop penetration into porous powder beds. *J Colloid Interface Sci*. 2002;253:353–366.
4. Hapgood KP, Litster JD, Smith R. Nucleation regime map for liquid bound granules. *AIChE J*. 2003;49:350–361.
5. Litster JD, Hapgood KP, Michaels JN, Sims A, Roberts M, Kameneni SK, Hsu T. Liquid distribution in wet granulation: dimensionless spray flux. *Powder Technol*. 2001,114:32–39.
6. Wauters PAL, van de Water R, Litster JD, Meesters GMH, Scarlett B. Growth and compaction behaviour of copper concentrate granules in a rotating drum. *Powder Technol*. 2002;124:230–237.
7. Hapgood KP, Litster JD, White ET, Mort PR, Jones DG. Dimensionless spray flux in wet granulation: Monte-Carlo simulations and experimental validation. *Powder Technol*. 2004,141:20–30.
8. Wildeboer WJ, Litster JD, Cameron IT. Modelling nucleation in wet granulation. *Chem Eng Sci*. 2005;60:3751–3761.
9. Hapgood K, Plank R, Zega J. Use of dimensionless spray flux to scale up a wet granulated product. In Proceedings of the World Congress on Particle Technology 4, Sydney, Australia, July 21–25, 2002.
10. Hapgood K, Jain S, Kline L, Moaddeb M, Zega J. Application of spray flux in scale-up of high shear wet granulation processes. In: AIChE Annual Meeting, San Francisco, November, 2003.
11. Ax K, Feise H, Sochon R, Hounslow M, Salman A. Influence of liquid binder dispersion on agglomeration in an intensive mixer. *Powder Technol*. 2008;179:190–194.
12. Litster JD, Hapgood KP, Michaels JN, Sims A, Roberts M, Kameneni SK. Scale-up of mixer granulators for effective liquid distribution. *Powder Technol*. 2002;124:272–280.
13. Plank R, Schenck L, Hapgood K, Zega J. Scale-up of a pharmaceutical high-shear wet granulation process using swept volume and dimensionless spray flux. In: American Institute of Chemical Engineers 2002 Annual Meeting (AICHE). 2002. Indianapolis, Indiana, USA.

14. Hapgood KP. Nucleation and binder dispersion in wet granulation, PhD thesis. Brisbane, Australia: University of Queensland, 2000.
15. Denesuk M, Smith GL, Zelinski BJJ, Kreidl NJ, Uhlmann DR. Capillary penetration of liquid droplets into porous materials. *J Colloid Interface Sci*. 1993;158:114–120.
16. Adamson AW, Gast AP. *Physical Chemistry of Surfaces*, 6th ed. New York: Wiley, 1997.
17. Middleman S. *Modelling Axisymmetric Flows: Dynamics of Films, Jets, and Drops*, Chapter 8. San Diego: Academic Press, 1995.
18. Wildeboer WJ, Koppendraaier E, Litster JD, Howes T, Meesters G. A novel nucleation apparatus for regime separated granulation. *Powder Technol*. 2007;171:96–105.